JOURNAL OF CATALYSIS 100, 103–117 (1986)

Study of a Tube-Wall Catalytic Methanation Reactor Using Coherent Anti-Stokes Raman Spectroscopy

W. A. ENGLAND,[1] D. H. W. GLASS, G. BRENNAN, AND D. A. GREENHALGH

Engineering Sciences Division, AERE Harwell, Didcot, Oxon OX11 0RA, United Kingdom

Received March 26, 1985; revised January 24, 1986

Coherent Anti-Stokes Raman Spectroscopy (CARS) has been used to obtain an axial CH_4 concentration profile in a laboratory catalytic tube-wall reactor. The resulting profile has been successfully compared with a theoretical model. An improved method for concentration analysis using CARS is presented, and future directions in the application of CARS to catalytic reactors are discussed.

INTRODUCTION

CARS (Coherent Anti-Stokes Raman Spectroscopy) is a laser-based spectroscopic technique which may be used to measure temperatures and concentrations in the gas phase. CARS is a technique which is rapidly being transferred from pure to applied research. Its versatility in important practical situations such as turbulent combustors (*1*), internal combustion engines (*2*), and plasmas (*3*) has already been demonstrated.

The aim of the present work was to study a simple, well-understood catalytic reactor using CARS spectroscopy. The resulting gas-phase concentrations measured by CARS could then be realistically compared with those predicted by theory. It was considered that this would provide a severe test of the CARS technique.

The optical arrangement for a typical CARS experiment is shown in Fig. 1. Three pulsed laser beams, two at frequency ω_l and one at ω_s are focussed and crossed at the measurement volume. If $(\omega_l - \omega_s)$ coincides with a Raman active transition of one of the components, a new laser-like anti-Stokes "signal" is generated such that $(\omega_l - \omega_s) = (\omega_{as} - \omega_l)$. The pencil-like directionality of the CARS signal beam facilitates discrimination against high levels of unwanted background light (e.g., luminescence and fluorescence). It also allows measurements to be made in confined areas.

By using a broad band ω_s, 100–200 cm^{-1} of molecular spectrum may be recorded from one laser pulse. The nature of the CARS experiment leads to the following special advantages of using CARS to study chemical reactors:

(1) Because CARS uses light beams, all measurements are carried out *in situ* without the use of mechanical sampling probes or thermocouples. This eliminates unquantifiable corrections due to probe perturbations caused by effects such as heat transfer, catalytic reactions, and flow disturbance. There is also no need for sample removal and conditioning prior to chemical analysis, as the measurement is made *in situ*.

(2) CARS is spatially precise. The CARS signal is only generated from the measurement volume, where the beams intersect; for our experiment this volume was typically a 10- to 20-mm-long cylinder 200 μm in diameter. For certain systems smaller volumes can be achieved.

(3) CARS is temporally precise since the signal is only produced during the ~10-ns

[1] Current address: B.P. Research Centre, Chertsey Road, Sunbury-on-Thames, Middlesex TW16 7LN, U.K.

0021-9517/86 $3.00

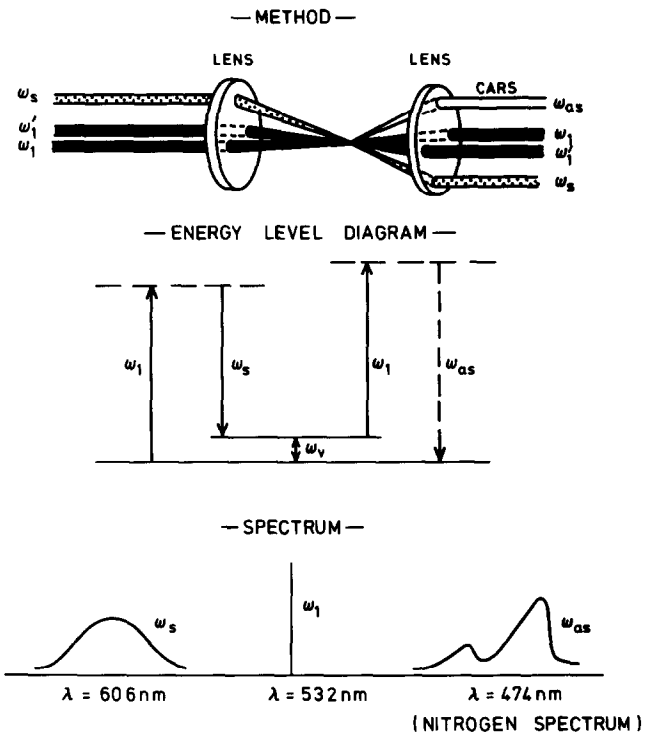

FIG. 1. Optical arrangement for a CARS experiment.

laser pulses. This is more than adequate to freeze any turbulence, so that the turbulence field may be evaluated by recording a series of "snapshots" of concentration or temperature at a chosen point.

The main optical requirement for CARS is the introduction of two windows connecting a narrow diameter line of sight. Concentrations are obtained from the experimental CARS data by fitting the concentration-dependent features of the spectra to theoretical models of spectral profiles. A similar method may be used for temperature measurements.

A previous study, which demonstrates the applicability of CARS to chemical reactors, has been reported by us (*4*). In this paper we have extended the concentration measurement technique, improved the reactor design, and succeeded in reconciling the observed data with models of the reactor.

The reaction selected for study was methanation. Methanation is the production of CH_4 from CO and H_2; it is catalysed by Ni/Al_2O_3 at temperatures from 175 to 400°C (*5–7*).

$$CO + 3H_2 \rightleftarrows CH_4 + H_2O; \qquad \Delta H^\circ_{298} = -206 \text{ kJ mol}^{-1}$$

The reaction is currently used to remove traces of CO from H_2 feedstocks in the Haber process. In the future it may be used to produce synthetic natural gas from coal-derived synthesis gas. Current reactors are of the fixed-bed type, but there is interest in using tube-wall or monolithic reactors in order to reduce pressure drops (*8, 9*).

We chose the methanation reaction to demonstrate the CARS technique because the spectroscopic properties of the components are well established. In addition, the CARS spectrum of CH_4 is simple and does not suffer overlap with other reactant or product molecules. Also the kinetics of the

reaction are sufficiently simple to permit comprehensive modelling, and are well established in the literature.

NOMENCLATURE

$\bar{A}$	preexponential factor (mol g^{-1} s^{-1} atm^{-1})
A	internal surface area of tube (m^2)
C	total concentration (mol m^{-3})
D	diffusivity (m^2 s^{-1})
E	activation energy (J mol^{-1})
I	intensity (arbitrary)
L	CARS interaction length (m)
M	minimisation function (mol^2 m^{-6})
N	molar flux (mol m^{-2} s^{-1})
r	radial coordinate (m)
R	gas constant (J mol^{-1} K^{-1})
$\bar{R}$	specific reaction rate (mol g^{-1} s^{-1})
$\bar{R}$	tube radius (m)
T	temperature (K)
V	max velocity (m s^{-1})
W	weight of catalyst (g)
x	mole fraction

Subscripts

A	component A
A0	initial value of component A
Ar	value in radial direction of component A
as	at anti-Stokes frequency (CARS)
B	at background position in CARS spectrum
calc	calculated
ijkl	polarization vectors of CARS beams
obs	observed
P	at peak position in CARS spectrum
s	at Stokes frequency (CARS)
1	at pump frequency (CARS)

Greek Symbols

Δ	CARS phase mismatch
Γ	molecular linewidth
$\chi^{(3)}$	third-order susceptibility (m^3 J^{-1})
ω	optical frequency (radians s^{-1})

METHODS

Catalyst preparation. The Ni/Al_2O_3 catalyst was prepared by an impregnation method. Cryogenic (75 × 6.3-mm-diameter, thin wall) stainless-steel tubes were coated with a Harwell Al_2O_3 sol. The coating was dried and then calcined at 450°C for 1 h and weighed as the oxide.

The coated tubes were next impregnated in 4 *M* $Ni(NO_3)_2$ solution for 2 min. After drying at 60°C the tubes were heated to 450°C to decompose the nitrates. The nickel loading was determined gravimetrically. The catalyst was activated before use by heating for 1 h at 500°C in pure H_2. By contrast, Vannice (*5*) used a H_2 reduction procedure as follows: 30 min at 120°C, 30 min at 260°C, and then 60 min at 450°C.

Two tubes were used for the CARS experiments; details of their nickel loadings are shown in Table 1.

Methanation reactor. The optically accessed methanation reactor is illustrated in Fig. 2. The 75-mm catalyst tube which comprises the reactor was held in the middle of the assembly by two "Swagelock" connectors. These connectors were drilled through

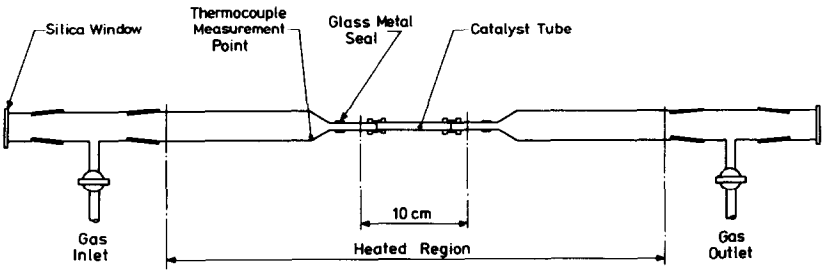

FIG. 2. Optically accessed tube-wall methanation reactor.

TABLE 1

Details of Coated Stainless-Steel Tubes Used for CARS Experiments

Tube No.	Weight of catalyst (mg)	Nickel loading (%)
1	189	11
2	224	9

with a 6.3-mm drill so that the laminar flow of gas was not disturbed by the stepped ridge in the middle of the connector. Glass–metal seals were used to join the rest of the apparatus to the gas handling equipment. Optical silica windows were attached to removable sections with epoxy seals.

The whole assembly, as indicated in Fig. 2, was maintained at 275 or 300°C in a Waytron scientific observation furnace. This furnace has a large constant temperature zone (±2 K) which is 200 mm long. The temperature of the catalyst was measured via a thermocouple near the end of the tapered Pyrex section (see Fig. 2).

The inlet gas composition was CO 4.5 mol%, H_2 13.5 mol%, and N_2 82.0 mol%, supplied from a premixed cylinder (i.e., a stoichiometric mixture of CO and H_2 diluted with N_2). Flow rates were set by a thermal mass flow controller calibrated against a bubble flow meter. Extra hydrogen could be blended by a second mass flow controller if required. The analysis of the exit stream was carried out with a Pye Unicam 204 gas chromatograph fitted with a thermal conductivity detector and a 2.5-m column containing molecular sieve 5A at 100°C. Peak areas were calculated with a LDC CI10 computing integrator.

Calibration. Standard mixtures of CH_4 in N_2 for calibrating the CARS measurements were prepared by using two mass flow controllers. These mixtures were checked with the gas chromatograph; the agreement was excellent. Table 2 compares the results of the mass flow controller and gas chromatographic analysis of the standard mixtures. The standard deviations were obtained from at least ten determinations of concentration.

CARS apparatus. A full description of the CARS apparatus has been reported in Ref. (*10*). The only significant changes were the use of a higher dispersion spectrograph, with a 1.7-m concave holographic grating, and the introduction of a half-wave plate in the ω_1 beams. The purpose of the half-wave plate is to rotate the plane of polarization of the ω_1 beams with respect to that of the ω_s beam. This improves the concentration analysis for reasons that will be discussed later.

The ω_1 pump beams were obtained from a JK Lasers, frequency-doubled, Nd/YAG laser with a total output power of 280 mJ, a linewidth of ~0.3 cm^{-1}, and a 10-Hz pulse repetition rate. Thirty percent of this was used to pump the 100 cm^{-1} FWHM wide broad-band dye laser centered at ω_s operating with DCM laser dye in ethanol. The DCM concentration was $\sim 1 \times 10^{-3}$ *M*. Because of the large shift between the lasing wavelength and absorption maximum of DCM there is virtually no dependence of the lasing maximum on DCM concentration. We chose to work with a nearly saturated solution of DCM in order to maximise the overall ω_s power.

We used a three-dimensional beam crossing arrangement known as "folded BOXCARS" (*11*) with a 0.5° half-crossing angle for the ω_1 beams. A 500-mm lens was used

TABLE 2

Results of Concentration Calibrations Based on CH_4/N_2 Mixtures. Experimental Standard Deviations are Shown in Parentheses

Mol% CH_4 in N_2 from flow controllers	Mol% CH_4 in N_2 from gas chromatography	$K^{1/2}$ value from CARS
4.12 (0.3)	4.28 (.16)	8.58 (.20)
2.61 (.02)	2.63 (.07)	5.73 (.11)
0.96 (.01)	0.98 (.06)	2.50 (.04)

to focus the laser beams at the desired point in the methanation reactor.

The dimensions of the region from which the CARS signal is generated (control volume) at the position of beam overlap were measured by translating a 1-mm-wide gas cell, filled with pure methane, across the control volume.

In order to measure the CH_4 concentration profile along the catalyst tube, the CARS control volume was kept fixed and the chemical reactor was moved by means of translation stage to an accuracy of ± 1 mm. For larger chemical reactors it would of course be more convenient to move the CARS control volumes by translating the lasers rather than the sample.

CARS concentration analysis. Figure 1 illustrates the beam crossing arrangement used for our experiments. The theory of CARS has been extensively reviewed elsewhere (*12, 13*). Briefly, the CARS process consists of the simultaneous excitation by intense electromagnetic fields (at ω_1 and ω_s) of the medium being studied. Under these conditions, nonlinearities in the response of the medium lead to the generation of a new field at a frequency such that $\omega_{as} = 2\omega_1 - \omega_s$ (i.e., the new field is shifted up in frequency by an amount equal to $(\omega_1 - \omega_s)$). The ω_{as} field generates a new laser-like signal beam which contains spectral information about the sample. Naturally $(\omega_1 - \omega_s)$ must be chosen to coincide with a specific Raman active transition of interest to the investigation. In our case by using a broad-band ω_s centred on the vibrational frequency of the methane symmetric stretch at 2914 cm^{-1} the entire spectrum could be recorded simultaneously.

The intensity of the CARS signal falling on the detector for monochromatic laser sources is given by

$$I(\omega_{as}) = [I(\omega_1)^2 I(\omega_s) L^2 \left|\chi^{(3)}_{ijkl}\right|^2 \frac{4\pi^2 \omega_{as}}{c^2 n_{as}} \frac{(\sin \Delta \cdot L/2)}{\Delta \cdot L/2}. \quad (1)$$

The third-power dependence of $I(\omega_{as})$ on $I(\omega_1)$ and $I(\omega_s)$ is clear from Eq. (1). The exact form of the observed spectrum only depends on the third-order susceptibility $|\chi^{(3)}_{ijkl}|^2$ and its variation with frequency. The main contributions of significance to CARS are shown below:

$$|\chi^{(3)}_{ijkl}|^2 = |\chi_{NR} + \chi' + i\chi''|^2 \quad (2)$$

χ' and χ'' comprise the resonant contributions to $\chi^{(3)}_{ijkl}$ which in our case are sharply concentrated around $(\omega_1 - \omega_s) = \omega_{methane}$. χ' and χ'' have the form of real and imaginary Lorentzians with linewidths Γ, while χ_{NR} is an effectively frequency-independent background term which may be thought of as arising from far off-resonant contributions from all the components in the matrix. For finite or multimode laser sources the spectra of the lasers must be correctly accounted for (*14, 15*). We have properly accounted for these factors in our method of data analysis which is discussed below. For simplicity we describe the fundamental properties of $\chi^{(3)}_{ijkl}$ for monochromatic sources, but the effect of laser linewidths should be borne in mind, particularly when physical modelling of CARS spectra is involved in data reduction. However, as our data analysis is based on direct calibration, the effects of laser linewidths are accounted for by the standardisation process.

Different molecules give rise to different values of χ_{NR}, the total value for any sample being the mole fraction weighted average of all the components. Most values of χ_{NR} for diatomics or triatomics are within a factor of 2 of each other (see Table 3). The presence of a buffer of nitrogen minimises the changes in χ_{NR} with the extent of the methanation reaction.

$$\chi_{NR}\,(\text{Matrix}) = \sum_i x_i \chi_{NR}(i). \quad (3)$$

The magnitude of the resonant part of $\chi^{(3)}_{ijkl}$ has a strong dependence on Γ, the molecular linewidth, since the susceptibility is inversely proportional to Γ. As discussed in our previous paper (*4*), Γ for a molecule

TABLE 3

Values for χ_{NR} Assumed in This Study

Molecule	$10^{17}\ \chi_{NR}$ ($m^3\ J^{-1}$)	Source
H_2	9.75	[a]
CO	10.13	Assumed to be the same as N_2
N_2	10.13	[a]
CH_4	22.13	[a]
H_2O	20.26	[b]

[a] Rado's values (*16*) multiplied by 2.5 as suggested by Ref. (*17*).

[b] Assumed to be $\sim 2\ \chi_{NR}(N_2)$ (*18*).

involved in a reaction may not be independent of the extent of reaction since Γ is matrix dependent and difficult to model in the absence of extensive physical data. The presence of a buffer (as in this experiment) has the effect of minimising the changes in Γ as the reaction proceeds. This has the effect of reducing any errors in concentration accuracy due to unaccounted changes in the molecular linewidths Γ.

Figure 3 shows a representative CARS spectrum of methane from the methanation reactor. The peak at the centre is due to methane, and the much broader feature from channel 200–800 is due principally to the nonresonant "background" susceptibility term in Eq. (2). The width of the nonresonant feature reflects the width of the broad-band dye laser centred at ω_S: it is seen to be $\sim 100\ cm^{-1}$ wide.

Figure 4 shows a series of spectra taken from the operating methanation reactor at different positions along the axis of the catalyst tube. The effect of changes in methane concentration is clear, the intensity of the methane peak changing relative to that of the nonresonant background.

We have discussed previously (*4*) a rapid and accurate method for analysing isothermal CARS spectra for concentration. This consists of forming the ratio of peak and "background" spectral intensities I_p and I_B.

$$K^{1/2} = (I_p/I_B)^{1/2} \tag{4}$$

which is linear with respect to concentration over certain ranges of concentration. Typical points for I_p and I_B are illustrated in Fig. 3. The position chosen for measuring I_B is arbitrary, but the linearity and slope of the $K^{1/2}$ versus concentration curve is de-

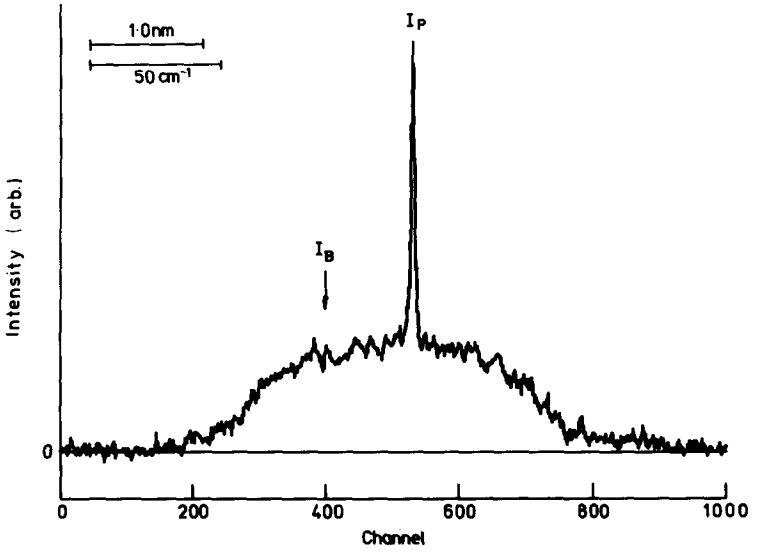

FIG. 3. Typical CARS spectrum of methane.

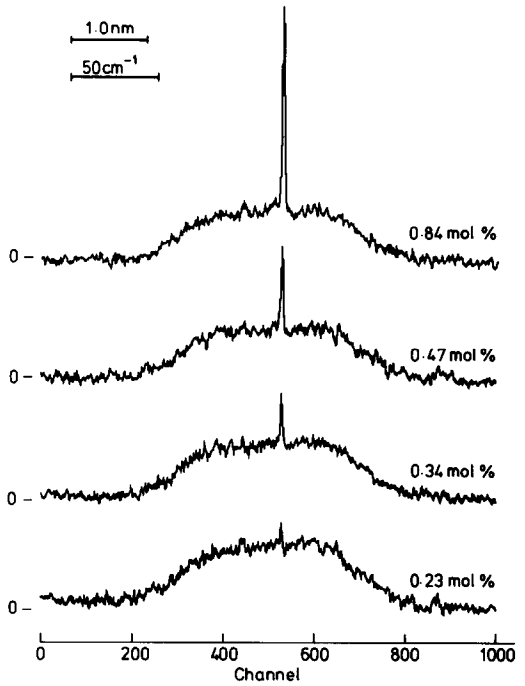

FIG. 4. Series of methane CARS spectra at different positions in the catalyst tube.

pendent on the frequency difference between the points chosen to measure I_p and I_B. If a theoretical model exists for a molecule, then the $K^{1/2}$ calibration curve may be calculated. However, as in the case of methane in a matrix of N_2, CO, H_2, H_2O, and CH_4 (where a model is not available) it is more effective to calibrate the CARS technique against standard gas mixtures. This was the approach used in this study.

For molecules such as CO, N_2, H_2O, and O_2 the range over which the $K^{1/2}$ calibration curve is linear is approximately 2–20%. In the case of CH_4, however, because of its very large resonant susceptibility this range is reduced to ~0.1–1% at 300°C. It is possible to circumvent this, however, by changing the relative polarization of the ω_1 beams with respect to the ω_s beam. This has the effect of changing the relative contribution from the resonant and nonresonant parts of $\chi^{(3)}_{ijkl}$ (*19*). By using this technique, which has previously been used in a different context (*2*), we were able to make concentration measurements, with a linear $K^{1/2}$ calibration curve, in the range 1–5% CH_4. The combination of the $K^{1/2}$ measurement technique with polarized CARS is very powerful because it allows one to "tune" the CARS experiment to the concentration range of interest for any particular molecule. CH_4 in N_2 mixtures, being convenient to prepare and analyse, were used to ensure that the CARS technique was giving a linear $K^{1/2}$ calibration curve over the desired concentration range (1–5% in our case). This was achieved by adjusting the beam polarization with a half-wave plate. During runs in the reactor, where the matrix was more complicated, the CARS technique was calibrated against the gas chromatographic analysis of the exit stream, the CARS measurement volume having been positioned past the end of the catalytic section of the reactor. This procedure has the advantage of eliminating the need for a small correction to account for χ_{NR} being different in the nitrogen calibration mixture and the methanation mixture, and for some of the matrix-dependent linewidth effects. It also corrects for any day to day fluctuations in the behaviour of the CARS apparatus. These could be due to changes in the temperature of the multiple order half-wave plate (or its orientation) or changes in the mutual coherence properties of the lasers (*20*).

Instead of forming $K^{1/2} = (I_p/I_B)$, it is more satisfactory to form the following ratio:

$$K^{1/2} = \bar{I}_p/I_B(\mathrm{Av}) \qquad (5)$$

$\bar{I}_p$ is the interpolated peak channel using four neighbouring channels around the peak channel. The interpolation is based on a finite difference method for a Lorentzian lineshape similar to that found in Ref. (*21*). I_B (Av) is the average value of the background CARS scattering over a range of typically 50 channels (or 12.6 cm^{-1}). Both the techniques reduce the noise in $K^{1/2}$ by including more statistically independent measurements in $K^{1/2}$. This improved esti-

mate of $K^{1/2}$ was used for all data reduction of experimental CARS spectra. In 500- and 10-shot spectra a small correction was made to the background level 500 channels away from the peak, to constrain it to be equal to an average value of 0 over 50 channels. This introduces a correction for the "dark noise" and background subtraction behaviour of our detector. The main source of noise is the instability in the dye laser, even when up to 500 spectra are summed together (*4*). Thus as the number of laser shots summed to produce a CARS spectrum is reduced, the uncertainty in derived concentrations is increased as the inverse of the square root of the number of laser shots. This will be demonstrated in the Results section.

Chemical reactor modelling. We investigated two approaches to modelling the tube-wall reactor. The first consisted of a detailed model which included the effect of radial mass transport in a laminar flow regime. The second was a plug flow model, based on an integration of the kinetic rate expression.

It was desirable to use both models so that we could establish under which conditions the simple plug flow model was valid. It was also necessary to calculate accurate radial concentration profiles in order to evaluate the effect of deviations of the CARS measurement volume from the principal axis of the tubular reactor.

The following assumptions were made in order to produce a detailed model of the tube-wall methanation reactor (first method):

(1) isothermal conditions;

(2) fully developed laminar flow along entire active catalyst section;

(3) negligible axial diffusion.

Under these conditions the following equation is valid:

$$\frac{D_A}{r}\frac{\partial}{\partial r}\left(r\frac{\partial}{\partial r}(Cx_A)\right) + V\left\{1 - \frac{r^2}{\bar{R}^2}\frac{\partial}{\partial z}(Cx_A)\right\} = 0. \quad (6)$$

The following boundary conditions were imposed:

(1) $x_A(r, 0) = x_{A0}$ (inlet condition)

(2) $\left.\frac{\partial x_A}{\partial r}\right|_{r=0} = 0$ (radial symmetry about axis)

(3) $N_{Ar}\Big|_{r=\bar{R}} = \tilde{R}_A\frac{W}{A}$. (reaction at wall)

The principal rate expression used was that proposed by Vannice (*5*) for a Ni/Al_2O_3 catalyst in the temperature range 240–280°C:

$$\tilde{R}_A = \bar{A}\exp\{-(E/RT)\}(P_{CO})^{-0.3}(P_{H_2})^{0.8}. \quad (7)$$

Equation (6) was solved using the Crank–Nicholson method for the reactants and products, with 100 radial and 150 axial points. The diffusivity D_A for each component was updated on each axial step using the Chapman–Enskog theory of multicomponent diffusion. The program also allows for the simultaneous solution of an energy balance similar to Eq. (6) for nonisothermal operation.

To validate the model and the solution method, the results from runs with a hypothetical, first-order reaction rate expression were checked against an analytical solution presented in Ref. (*22*) which included axial diffusion. Both diffusion and kinetic control were simulated by varying the rate constant, and good agreement was obtained in both cases.

The neglect of axial diffusion in our model may be justified by its small magnitude in comparison to radial diffusion. Under the conditions of our experiment, it is 3% or less of the radial term. This may be understood as a combination of two factors. First, the presence of a nitrogen diluent reduces the absolute magnitude of the concentration gradient, and second, the absence of a conventional catalyst packing eliminates an important source of axial dispersion. The excellent agreement with the experimental concentration profile (pre-

sented later), and the validation with an analytical model including axial dispersion, further justifies our neglect of this effect in our model.

In order to compare experimentally obtained concentration profiles with those predicted by theory, a nonlinear least-squares fitting program VA05A (from the Harwell Subroutine Library) was employed to adjust various parameters to optimise agreement between observed and calculated concentration profiles. The adjustable parameters were the preexponential factor, $\bar{A}$, and an offset parameter which allowed for any small error in measuring the position of the CARS beam cross-over with respect to the focusing lens. Since the CARS signal is not generated from a single geometrical point in space, the finite size of the control volume was included in the model. The observed CARS signal was assumed to be generated from a control volume of dimensions determined experimentally to be 11 ± 3 mm FWHM with a Gaussian form. This was then convoluted with the calculated axial concentrations profile to yield the calculated profile as observed by CARS.

In addition to the model described above, a second model, using a one-dimensional plug flow assumption was also written to compare with the fuller description of Eqs. (6) and (7). The computer program, together with a listing, has been described in Ref. (*23*).

In practice, for the catalyst which we used, under the operating conditions of the experiment, the detailed model and the plug flow model gave identical results. The radial concentration profile was negligible. We were therefore able confidently to use the plug flow model for our data reduction.

RESULTS AND DISCUSSION

The results of the methane in nitrogen calibration at 275°C are shown in Fig. 5. The polarization was such as to give nearly complete cancellation of χ (resonant). The curve is an excellent straight line with an intercept of 0.75 on the $K^{1/2}$ axis. The $K^{1/2}$ point plotted for zero methane concentration corresponds to the "raw" dye laser profile as mirrored by the nonresonant susceptibility. Spectral modelling shows that the intercept of a $K^{1/2}$/concentration graph does not necessarily occur at the point

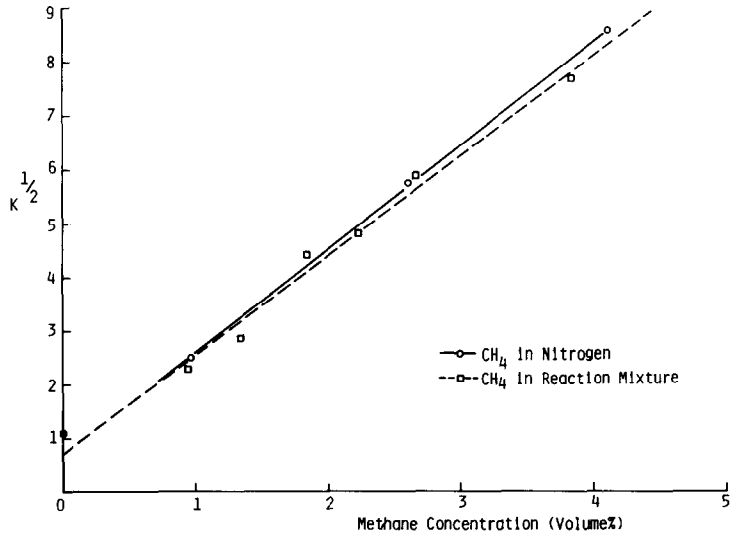

FIG. 5. Results of CARS calibration of CH_4 in N_2 and in the reaction mixture.

given by the "raw" dye laser spectrum. Furthermore, at lower concentrations, the slope of the curve reduces for the last portion of the concentration range. The exact point where this occurs can only be found by calibration (or calculation where sufficient data exist). In our case this would only affect points below 1% and the correction would be relatively modest since our intercept (0.75) is close to the "raw" dye laser value (1.05).

Figure 5 also shows the corresponding calibration curve for methane in the product stream of the methanation reactor (i.e., when the CARS measurement volume was positioned past the end of the catalytic section of the reactor and the exit stream concentration was measured by gas chromatography). This curve also gives an excellent straight line, but with a higher degree of scatter on the points. This is ascribed to small changes in the day to day performance of the CARS apparatus. (The methane in nitrogen calibration was completed in half a day). A least-squares fit to the two curves shows a change in slope of 4.7%. This may be attributed to the higher value of χ_{NR} in the product stream compared to pure N_2. A calculation according to Eq. (3) shows that the expected slope change is 2.3%, reasonably close to the value observed given the precision of the experiment.

The excellent agreement of the calibrations in nitrogen and the reaction mixture shows that variations in parameters such as molecular linewidth, Γ, and χ_{NR} with the extent of the methanation reaction are insignificant.

Concentrations from runs involving the methanation reactor were deduced from the appropriate calibration point taken at a point past the catalytic tube, assuming the intercept with the $K^{1/2}$ axis from Fig. 5.

It should be noted that without the use of polarized CARS we would only have been able to measure methane concentrations at 275°C between circa 0.1 and 1% with a suitable degree of accuracy. This was established by carrying out calibration runs at this temperature, using methane in nitrogen.

As mentioned earlier, the precision of a CARS concentration measurement is expected to improve in proportion to the square root of the number of spectra summed together. We investigated this effect experimentally by making multiple measurements of different exposure times during our calibration runs. Concentrations were deduced for each individual measurement, and standard deviations calculated from the data thus produced. The results are shown in Table 4 for spectra produced by summing 500, 10, or 1 firings of the laser (i.e., exposure times of 50, 1, and 0.1 s).

TABLE 4

Experimental Precision of CARS Concentration Measurements for Different Exposure Times

Number of shots	Concentration[a] volume (%)	Standard deviation in derived CARS concentration volume (%)	Relative standard deviation (%)
500	4.12	0.102	2.5
500	2.61	0.058	2.2
500	0.96	0.019	2.0
10	2.61	0.294	11
1	2.61	0.408	16

[a] As measured by mass flow controllers.

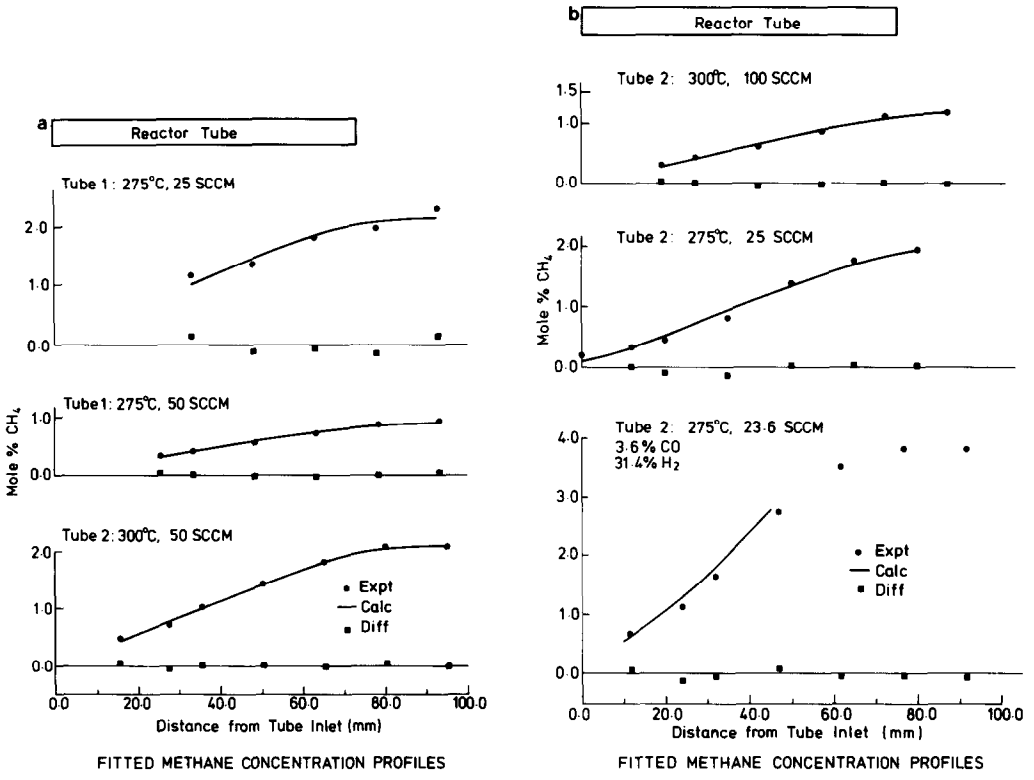

FIG. 6. (a) Observed and (b) calculated CH_4 concentration profiles from the methanation reactor.

The main source of noise in the derived concentrations arises from the instabilities in the broad-band dye laser; since $\bar{I}_p$ (Eq. (5)) is measured from only a few channels it is very sensitive to changes in the locally "ragged" dye laser profile. Molecules with broader spectral shapes (e.g., most diatomics except H_2 and most triatomics except CO_2) would be less sensitive to dye laser noise because $\bar{I}_p$ could be obtained by an average over more channels.

Figures 6a and b summarise the results from the tube-wall reactor. The points represent the experimentally measured CH_4 concentrations using the $K^{1/2}$ method of Eq. (5) and exposure times of 50 s (500 shots). The continuous line was calculated using the computer model described above and in Ref. (*23*). The kinetic model of Vannice (*5*) was used for this part of the study [see Eq. (7)]. As may be seen from the diagram, the agreement between theory and experiment is extremely good. There do not appear to be any systematic errors as shown by the random nature of the difference plots. This is a convincing demonstration of the accuracy and precision of the CARS technique for concentration measurements.

The values for the derived parameters are shown in Table 5 both for Vannice's kinetic model and that due to Hayes, Thomas and Hayes (*24*) who studied the range 260–300°C at 1 atm pressure:

$$\bar{R}_A = 8.69 \exp\left(\frac{-9270}{T}\right) P_{H_2}^{1.27} P_{CO}^{-0.87} P_{H_2O}^{-0.13}. \quad (8)$$

The former model gives a less constant value for the preexponential factor than the latter, indicating that the activation energy of Hayes *et al.* (78 kJ mol^{-1}) is closer to that

TABLE 5

Derived Preexponential Factors from the Least-Squares Fitting of the CH_4 Concentration Profiles

This study				
Temperature (°C)	Flow rate (SCCM)	Tube No.	Preexponential factors	
			mol g^{-1} s^{-1} $atm^{0.5}$ [a]	mol g^{-1} s^{-1} $bar^{-0.27}$ [b]
275	25	1	2.86×10^6	23.8
275	25	2	2.18×10^6	18.3
275	50	1	2.22×10^6	16.5
300	50	2	1.40×10^6	17.9
300	100	2	1.58×10^6	19.3
275	24	2	1.86×10^6	7.46
Literature				
260–300	—	—	—	8.79
240–280	—	—	5.6×10^4	—

[a] Vannice's model (5) (extrapolated to 11% loading).
[b] Hayes *et al.* (24).

of our catalyst than Vannice's (120 kJ mol^{-1}). Our preexponential factor at 300°C is a factor of ~2 greater than that of Hayes *et al.* Our preexponential factor is ~25 times greater than that reported by Vannice, after extrapolating Vannice's 5% Ni loading to the 11% loading used by us. The discrepancies in the preexponential factors are probably due to a number of factors connected with the physical properties of the catalysts, which depend on the details of their preparations. Parameters such as catalyst dispersion, particle size, and the nature of the catalyst support have a marked effect on the activity of the catalyst.

Both the catalysts used by Vannice, and by Hayes *et al.* were prepared by the incipient wetness technique. Vannice's catalyst composition was 5% Ni on Al_2O_3 whereas Hayes *et al.* used 9% Ni on Al_2O_3 promoted with 1.5% Pt. There were also slight differences in the H_2 reduction steps, as described in the experimental section. Hayes et al. used a reduction procedure similar to Vannice, but without the step at 120°C.

Under the conditions of our experiments, the fully detailed model, including radial diffusive mass transfer, laminar flow and a heat balance (ie Eq. (6) and related boundary conditions), gave identical results to a simpler plug flow model. Since the plug flow model ran 50 times faster than the fuller model on the computer, we used the plug flow model for all our work. This indicates that under the conditions used by us, diffusive resistance was negligible compared to kinetic resistance.

The sensitivity of the least-squares fit to the details of the kinetic model was assessed by making small stepwise changes to the nature of the rate expression and noting the effect on the minimisation functions, M:

$$M = \sum_i (x_{obs} - x_{calc})^2. \qquad (9)$$

Since, for all but one of our runs, we were operating with the same stoichiometric mixture of CO and H_2 diluted with N_2 our model was only sensitive to the *overall* reaction order in Vannice's model (Eq. (7)) since P_{CO} is always one-third of P_{H_2}. Vannice's model thus may be thought of as hav-

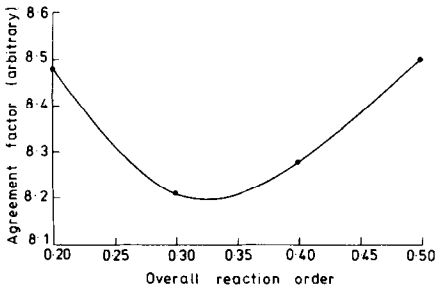

FIG. 7. Dependence of the least-squares minimisation factor on the rate order.

ing an overall order of 0.5, while that of Hayes *et al.* has an overall order (neglecting the inhibition by H_2O) of 0.4.

The sensitivity of our model to reaction order was assessed by performing least-squares fits with values for the reaction order of 0.2, 0.3, 0.4, and 0.5 and noting the change in the least squares minimisation function M. The best model should be represented by the smallest value of M. The result of this procedure is shown in Fig. 7 which has a minimum at a rate order of -0.32. In other words, our data suggests better compliance with the model of Hayes *et al.* (*24*) than that of Vannice (*5*).

It should be realised, however, that with fractional orders in rate expressions small changes in the value of the order do not make very significant changes to the rate of reaction or the shape of the axial concentration profile. This is illustrated in Fig. 8 where profiles for the same overall conversions are presented, calculated for the two different rate expressions. The small difference between them is basically one of slope: the model of Hayes *et al.* has a lower slope due to the lower overall order with respect to CO and H_2 and the inclusion of an H_2O inhibition term.

By contrast, one experiment was performed with excess H_2 present in the input stream to the catalytic reactor. The result is shown in Fig. 6b (lower graph). The calculation was only performed in the concentration range for which the rate expressions are valid. The distinct upward curvature of the experimental points and fitted curve in the early stages of the reactions is a direct result of the change in effective order to one dominated by the negative order with respect to CO. This negative order is seen in both rate expressions, but Hayes *et al.* have an order of -0.87 whereas Vannice gives -0.3. We investigated the effect of changing the CO order on the minimisation function by performing least-squares fits

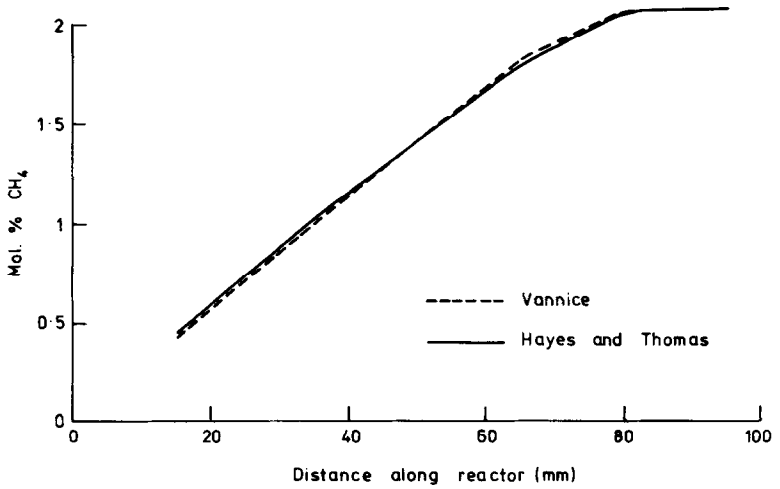

FIG. 8. Comparison of the axial methane concentration profiles calculated using the rate expressions of Vannice (*5*) and Hayes *et al.* (*24*).

with an overall order of 0.4 and a varying CO order. This revealed improved fits as the CO order changed from −0.3 to −0.87; beyond this there was little decrease in the value of M.

To summarise the results of the kinetic modelling, we have shown that both kinetic models give excellent fits, but there is evidence that the model of Hayes *et al.* represents the behaviour of our catalyst better than that of Vannice.

It is encouraging that CARS concentration profiles give the same kinetic parameters as conventional microreactor approaches. The data content of a concentration profile is obviously higher than a single total conversion measurement for a given tube length. Operationally speaking, a profile with 10 points in it represents a set of conventional total conversion measurements on 10 different tube lengths taken simultaneously.

CONCLUSIONS

Isothermal CARS measurements of CH_4 concentration profiles have been successfully made and interpreted in a tube-wall catalytic methanation reactor. An improved variant of the "$K^{1/2}$ ratio" concentration analysis procedure (*4*). making use of partial polarization cancellation, was used to "tailor" the experiment to the desired concentration range. The direct *"in situ"* calibration of CARS spectra for concentration analysis (without the need for the development of complex physical modelling of spectral shapes) has been reported for the first time. This will pave the way for future studies on a far wider variety of molecules than was previously possible. A similar method for temperatures has been reported by Akhmanov *et al.* (*25*).

Having demonstrated the use of CARS concentration measurements on a laboratory reactor we feel that the future direction of CARS lies increasingly towards systems in which heat and mass transfer effects are important. In other words CARS will be increasingly applied to industrial- and pilot-scale plants (*26*) as well as to laboratory systems designed to isolate particular features of interest to full-scale plants. We are confident that CARS is in a position to provide valuable design and operating data to the chemical reactor designer and operator.

Possible future directions for the use of CARS in catalytic reactor studies include the following:

(1) The study of turbulent and/or non-isothermal tube-wall catalytic reactors to characterise heat and mass transfer effects.
(2) The study of monolithic reactors, on a channel by channel basis.
(3) The study of oscillating chemical reactors.
(4) The study of reactions over precious metal gauzes, where temperature and concentration profiles above and below the catalyst could be studied.

ACKNOWLEDGMENTS

We acknowledge useful discussions with Professor W. J. Thomas and his group at the School of Chemical Engineering of the University of Bath, and we are grateful to members of the Harwell Catalyst Unit for advice on catalyst preparation. We acknowledge the support of the Materials, Chemicals and Vehicles Requirements Board of the UK Department of Trade and Industry.

REFERENCES

1. Greenhalgh, D. A., Porter, F. M., and England, W. A., Comb. Flame, **49,** 171 (1983).
2. Stenhouse, I. A., Williams, D. R., Cole, J. B., and Swords, M. D., *Appl. Opt.* **18,** 3819 (1979).
3. Péalat, M., Taran, J. P. E., Taillet, E., Bacak, M., and Bruneteau, A. B., *J. Appl. Phys.* **52,** 2687 (1981).
4. England, W. A., Milne, J. M., Jenny, S. N., and Greenhalgh, D. A., *Appl. Spectrosc.* **38,** 867 (1984).
5. Vannice, M. A., *J. Catal.* **37,** 462 (1975).
6. Vannice, M. A., *J. Catal.* **44,** 152 (1976).
7. Sughrue, E. L., and Bartholomew, C. H. *Appl. Catal.* **2,** 239 (1982).
8. Jarvi, G. A., Mayo, K. B., and Bartholomew, C. H., *Chem. Eng. Commun.* **4,** 325 (1980).
9. Pennline, H. W., Schehl, R. R., and Haynes, W. P., *Ind. Eng. Chem., Process. Des. Dev.* **18,** 156 (1979).
10. Greenhalgh, D. A., and England, W. A., AERE Harwell Report No. R10282 (1982).

11. Eckbreth, A. C., *Appl. Phys. Lett.* **32,** 421 (1978).
12. Hall, R. J., and Eckbreth, A. C., *in* "Laser Applications" (J. F. Ready and R. K. Erf, Eds.), Vol. 5, pp. 213–309. Academic Press, New York, 1984.
13. Nibler, J. W., and Knighten, G. B., *in* "Topics in Current Physics" (A. Weber Ed.), Chap. 7, pp. 223–299. Springer-Verlag, 1979.
14. Yuratich, M. A., *Mol. Phys.* **38,** 625 (1979).
15. Teets, R. E., *Opt. Lett.* **9,** 226 (1984).
16. Rado, W. G., *Appl. Phys. Lett.* **11,** 123 (1968).
17. Eckbreth, A. C., and Hall, R. J., *Combust. Sci. Technol.* **25,** 175 (1981).
18. Greenhalgh, D. A., Hall, R. J., Porter, F. M., and England, W. A., *J. Raman Spectrosc.* **15,** 71 (1984).
19. Rahn, L. A., Zych, L. J., and Mattern, P. C., Sandia Combustion Research Facility, Annual Report 1979.
20. Rahn, L. A., Farrow, R. C., and Lucht, R. P., *Opt. Lett.* **9,** 223 (1984).
21. Zimmerman, W., *Rev. Sci. Instrum.* **32,** 1063 (1961).
22. Baron, T., Manning, W. R., and Johnstone, H. F., *Chem. Eng. Prog.* **48,** 125 (1952).
23. Glass, D., Brennan, G., England, W. A., and Greenhalgh, D. A., AERE Report No. R11396 (1984).
24. Hayes, R. E., Thomas, W. J., and Hayes, K. E., *J. Catal.* **92,** 312 (1985).
25. Akhmanov, S. A., Gladkov, S. M., Karimov, M. G., Koroteev, N. I., Zadkov, V. N., and Marowsky, G., *IEEE J. Quantum Electron.* **QE-20,** 424 (1984).
26. England, W. A., and Greenhalgh, D. A., *in* "Proceedings, VIIIth ISCRE" (Edinburgh 1984), p. 263. Pergamon, Oxford, 1984.